Numerical Analysis of LM MHD Flows in Splitting Ducts under a Uniform Magnetic Field

Yang Luo, Chang Nyung Kim*, Xuejiao Xiao

***Abstract* — In the present study, three-dimensional liquid-metal magnetohydrodynamic splitting flows in a duct with one inflow channel and two outflow channels are numerically investigated. A uniform magnetic field is applied, which forms an angle θ with the x-axis. The numerical calculation is performed by using CFX code, with a structured grid system chosen after a series of mesh independence tests. Also, the interdependency among the current, fluid velocity, electric potential and pressure distribution is elucidated in order to describe the electromagnetic characteristics of the liquid-metal flows. The result shows that higher velocities are observed in the side layers and the pressure gradient in the inflow channel is the largest. Meanwhile, the current flows diagonally due to the applied magnetic field.**

Keywords: liquid metal flow, magnetohydrodynamic, numerical examination, splitting duct

I. Introduction

A liquid metal (LM) Magnetohydrodynamic (MHD) flow is an interesting topic in engineering applications, especially important in the design of liquid-metal (LM) cooling system of fusion reactors. The interaction between the magnetic field and moving liquid metal leads to diversification of MHD phenomena. In the fusion blanket the liquid metal can serve both as breeder material and as coolant. Nowadays, numerous works have been carried out on liquid metal (LM) magnetohydrodynamic (MHD) flows in the fusion blanket.

Many experimental methods have been performed to analyze the features of liquid metal MHD flows in ducts. A series of experiments on MHD flows in a prototypical three-channel manifold system relevant to the Dual Coolant Lead Lithium (DCLL) blanket were performed by Messadek et al. [1]. Stieglitz [2] analyzed the flow in right-angle bends by experimental approach, in which a flow in a direction perpendicular to the magnetic field is changed to one that is parallel to the field. Many different experiments on LM MHD flows were performed by Kirillov et al. [3], and the recent progresses on liquid metal magnetohydrodynamic duct flows was discussed in this study.

The characteristics of the LM MHD flows have been investigated by numerous mathematical methods. Cuevas et al. [4] mathematically studied the fully developed liquid-metal MHD flows in rectangular ducts for laminar and turbulent flows. Aleksandrova and Molokov [5] obtained a mathematical solution of two-dimensional MHD flows in a duct with sudden expansions and contractions, and the results show that the electromagnetic force is well balanced with the inertia force in the parallel layer. Siddheshwar [6] adopted a mathematical method with an inertialess approximation, which allowed the analysis of MHD flows in a viscoelatic liquid easier.

In order to investigate the characteristics of three-dimensional LM MHD flow well, numerical studies for three dimensional MHD flows have been lately performed with various codes developed by respective researchers. Zhou et al. [7] employed structural collocated grids in their computational code that can predict LM MHD flows in rectangular ducts. Piazza and Buhler [8] used CFX code to present a numerical simulation of buoyancy-driven magnetohydrodynamic flows in a duct. Mao and Pan [9] analyzed a three-dimensional LM MHD duct flow by numerical method. Reimann et al. [10] performed the assessment of pressure drop in components where strong three-dimensional electric current is induced, together with the multi-channel effects in LM MHD duct flows.

Though many analytic, experimental and numerical studies on MHD duct flows have been recently performed, detailed flow characteristics of LM MHD flows in a splitting duct under a uniform magnetic field, which forms an angle ($\theta = 30^0$) with the x-axis, have not been nearly investigated. In the present study, three-dimensional MHD flows in a splitting duct are numerically investigated by using CFX code. The characteristics of the velocity, current, electric potential and pressure gradient of MHD flows in splitting ducts are analyzed in this study.

II. Problem Formulation and Solution Method

A. Geometry, magnetic field and materials

In the current study, a steady-state, constant-property and laminar flows of an incompressible and electrically conducting liquid-metal (Pb-17Li) fluid under an external magnetic field is investigated. The geometry of the duct is shown in Fig. 1. A uniform magnetic field B_0 = 0.9632 T corresponding to Hartmann number 1000 is applied, which

Manuscript received April 17, 2018; revised April 19, 2018. This research was supported by National R&D Program through the National Research Foundation of Korea (NRF) funded by the Ministry of Future Creation (2015M1A7A1A02050613).

Yang Luo is with the Mechanical Engineering department, Graduate School, Kyung Hee University, Yong-in, Republic of Korea

Chang Nyung Kim is with the Mechanical Engineering department, College of Engineering, Kyung Hee University, Yong-in, Republic of Korea (e-mail: cnkim@khu.ac.kr).

Xuejiao Xiao is with the Mechanical Engineering department, Graduate School, Kyung Hee University, Yong-in, Republic of Korea

forms an angle ($\theta = 30^0$) with the x-axis. The Hartmann number can be written as follows:

Hartmann number $M = B_0 L\sqrt{\sigma_f / \mu_f}$ (1)

where σ_f is the electrical conductivity of the fluid, B_0 is the magnetic field strength, L is the characteristic length, (i.e., 0.05 m, the half-length of a side of the flow conduit cross-section), μ_f is the dynamic viscosity of the fluid, respectively. The properties of the working fluid and the wall are given in Table 1.

B. Governing equations

A steady-state, incompressible, constant-property, laminar, LM MHD flow of electrically-conducting liquid metal under a uniform magnetic field is governed by the following equations:

Conservation of mass $\nabla \cdot \vec{u} = 0$ (2)

Equation of motion $\rho\vec{u} \cdot \nabla\vec{u} = -\nabla p + \mu\nabla^2\vec{u} + \vec{J} \times \vec{B}$ (3)

Conservation of the charge $\nabla \cdot \vec{J} = 0$ (4)

Ohm's law $\vec{J} = \sigma(-\nabla\phi + \vec{u} \times \vec{B})$ (5)

where, $\vec{u}$ is the velocity vector, ρ is the fluid density, p is the pressure, μ is the dynamic viscosity, $\vec{J}$ is the current density vector, σ is electric conductivity, $\vec{B}$ is the magnetic field intensity vector and ϕ is the electric potential, respectively.

The combination of Eq. (4) and Eq. (5) gives the following equation of Poisson type for the electric potential.

$\nabla^2\phi = \nabla \cdot (\vec{u} \times \vec{B})$ (6)

Therefore, for a liquid metal magnetohydrodynamic flow, the variables of the pressure, velocity and electric potential can be solved by Eqs. (2), (3), and (6). It can be noted that the velocity in the duct region is to be zero, and that the electric potential in the fluid and solid (i.e., duct) region is solved in the 'conjugated manner', needing no boundary condition at the interface of the fluid and solid.

C. Boundary conditions

At the fluid-solid interface no slip condition is applied. At the inlet, a uniform velocity u = 0.01 m/s is given, which gives the Reynolds number ($Re = \rho u L \mu^{-1}$) 2660. And, the pressure value at the outlets is considered to be zero. It is presumed that the whole system including the fluid and duct walls are electrically insulated from the outside.

D. Numerical method

The present study uses a structure grid system of around 4,150,852 grids for the simulation. Finer grids are employed in the fluid region near the walls and in the transition segment. For discretized equations, Multigrid-accelerated Incomplete Lower Upper factorization technique [11] is used. Rhie-Chow Interpolation method [12] is employed for the pressure-velocity coupling. Under-relaxation is utilized in the iteration procedure for the coupled governing equations. The second-order upwind scheme is applied to discretize the convective terms, and the central difference scheme is adopted for diffusion terms. For the validation of the present numerical modelling with the use of CFX code, Ref. [13] can be consulted.

III. RESULTS AND DISCUSSIONS

Fig. 2 shows the distribution of axial velocity in the z-x plane at y = 0.5 m, where higher axial velocities are observed in the side layers, forming 'M-shaped' profile. The distributions of the current density and electric potential in the z-x plane at y = 0.5 m are shown in Fig. 3. The current flows from the right side to the left side in the fluid region, and then returns to the right side wall through the duct walls. As can be seen in Fig. 3(b), a higher electric potential is induced in the fluid region near the left side wall, while a lower electric potential is observed in the fluid region near the right side wall.

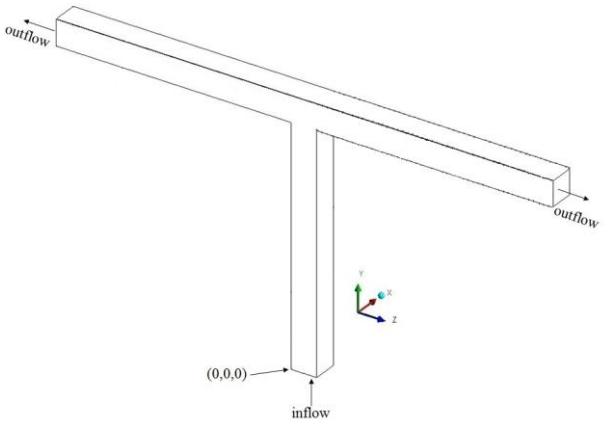

(a) Bird's eye view

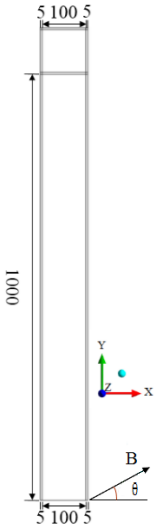

(b) Side view

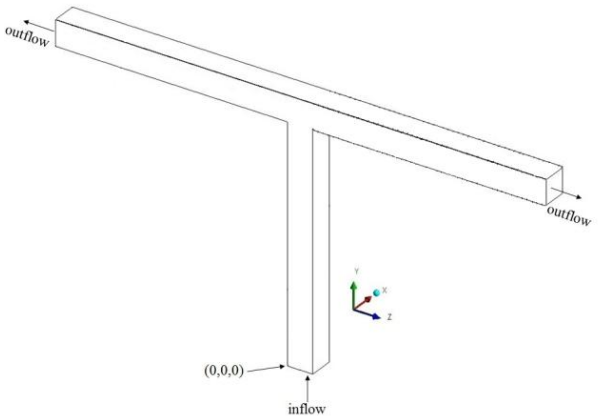

(c) Front view

Fig. 1 Duct geometry, coordinate system and an applied magnetic field (unit: mm).

ISBN: 978-988-14048-9-3
ISSN: 2078-0958 (Print); ISSN: 2078-0966 (Online)

TABLE I
MATERIAL PROPERTIES

	Density (kg/m^3)	Kinematic viscosity (m^2/s)	Electric conductivity (S/m)
Liquid metal (Pb-17Li)	9500	0.188×10^{-6}	7.7×10^5
Wall			10^7

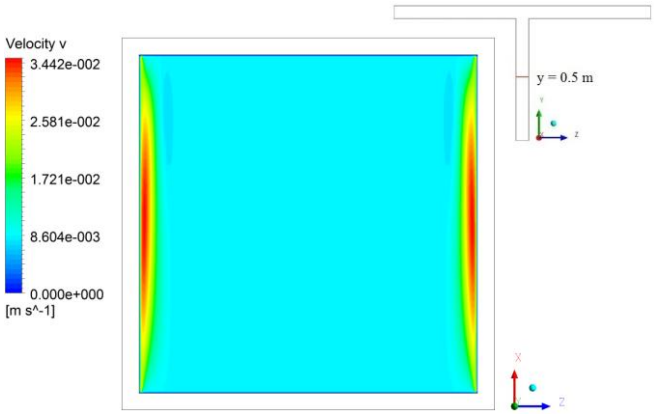

Fig. 2 Distribution of the axial velocity in the z-x plane at y = 0.5 m.

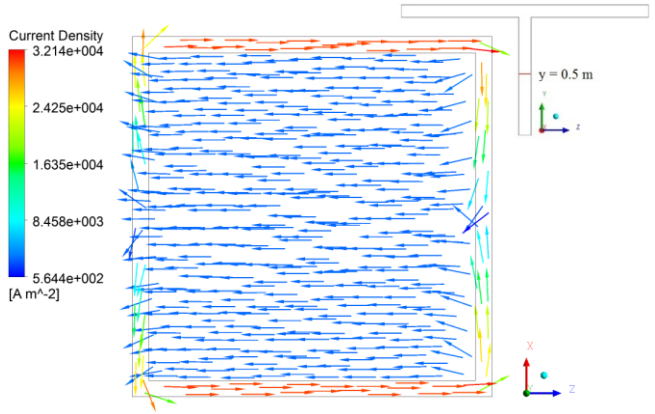

(a) Current density

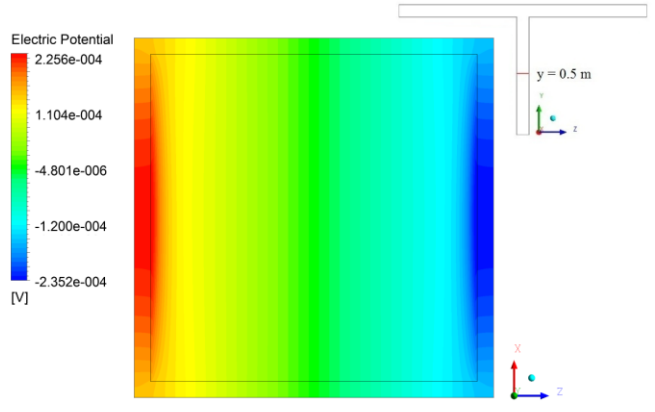

(b) Electric potential

Fig. 3 Current density and electric potential in the z-x plane at y = 0.5 m.

Fig. 4 displays the velocity distributions in the mid y-z plane (at x = 0.055 m) around the transition segment. The fluid flows in the y-direction in the inflow channel, and then the fluid changes the direction in the transition segment to flow in the positive and negative z-direction in the right and left outflow channels, respectively. Higher velocities are observed in the fluid region above the left and right edges. As shown in the Fig. 4(b), a crescent of high velocity is observed in fluid region near the left and right edges of the transition segment.

The distributions of the current density and electric potential in the mid y-z plane at x = 0.055 m around the transition segment are shown in Fig. 5. In the inflow channel, the current heads to the left wall in the fluid region. In the transition segment, the current flows in a round way radially from the region near the right edge to that near the left edge. In the right outflow channel, the current heads upward, while in the left outflow channel it heads downward. As can be seen in Fig. 5(b), higher electric potential is formed in the fluid region near the left side wall of the inflow channel, and near the bottom wall of the left outflow channel. While lower electric potential is observed in the fluid region near the right side wall of the inflow channel, and near the bottom wall of the right outflow channel.

The x-directional velocities in the planes of the entrance of the right outflow channel (i.e., that located at z = 1.005 m) is shown in Fig. 6. In the fluid region near the top wall, the highest x-directional velocity is obtained near the right edge, while the lowest x-directional velocity is observed in the fluid region near the left edge of bottom wall. Since the applied magnetic field forms an angle with the x-axis, the induced velocity forms the same angle with the x-axis in Fig. 6.

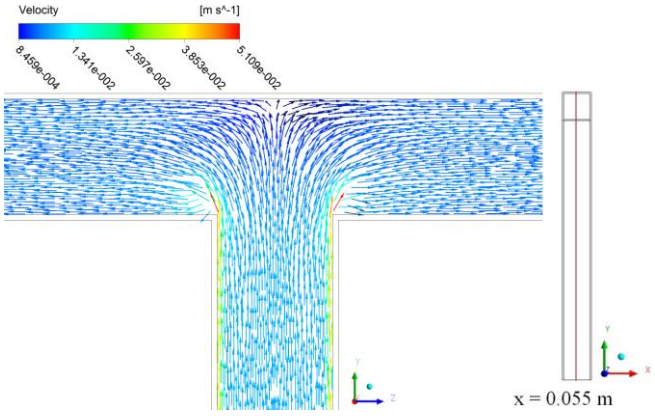

(a) Velocity vector

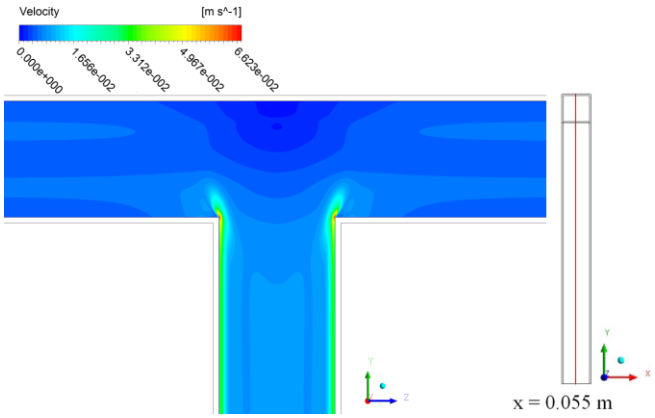

(b) Velocity distribution

Fig. 4 Plane velocities in the mid y-z plane at x = 0.055 m around the transition segment

ISBN: 978-988-14048-9-3
ISSN: 2078-0958 (Print); ISSN: 2078-0966 (Online)

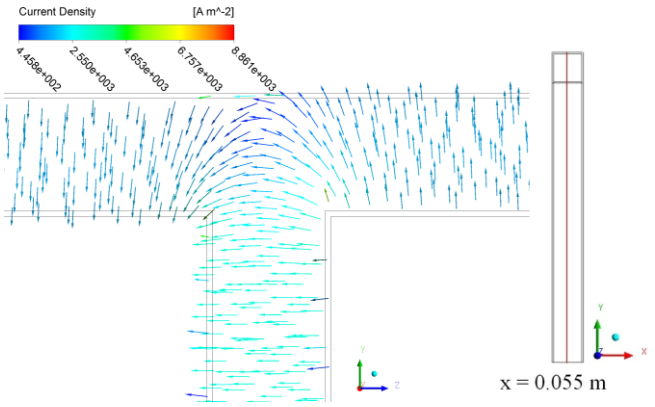

(a) Current density

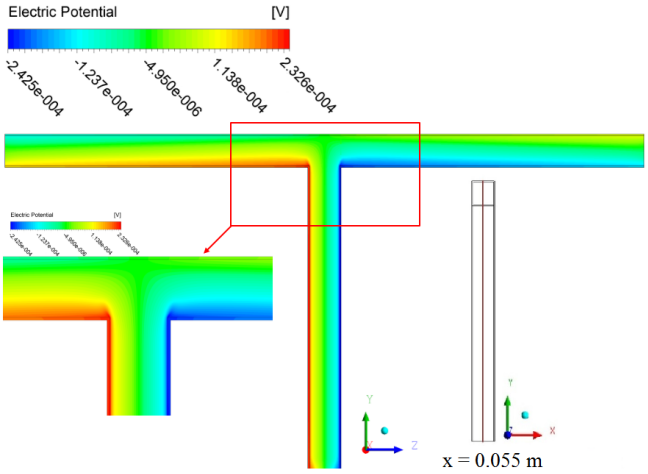

(b) Electric potential

Fig. 5 Current density and electric potential in the mid y-z plane at x = 0.055 m around the transition segment.

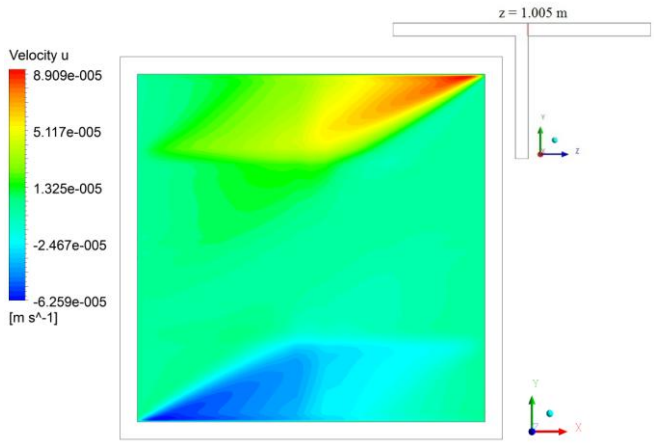

Fig. 6 X-directional velocity at z = 1.005 m.

Fig. 7 shows the distributions of the current density and electric potential in the x-y plane at z = -0.5 m. The current flows diagonally from the region near the left edge of top wall to that near the right edge of bottom wall, then returns to the left edge of top wall through the duct walls. Meanwhile, higher electric potential is observed in the fluid region near the right edge of bottom wall, and lower electric potential is obtained in the fluid region near the left edge of top wall.

The pressure distributions along the imaginary lines are displayed in Fig. 8. As shown, the pressure almost linearly

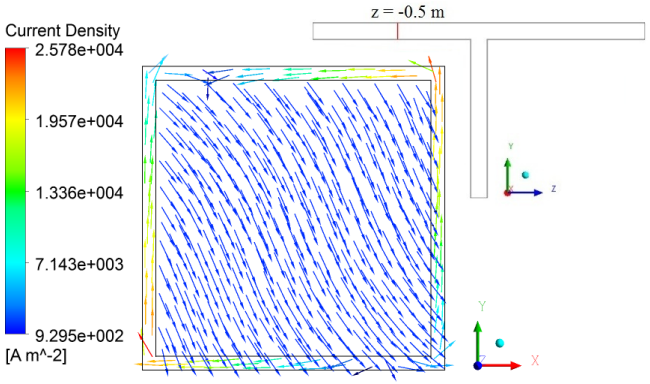

(a) Current density

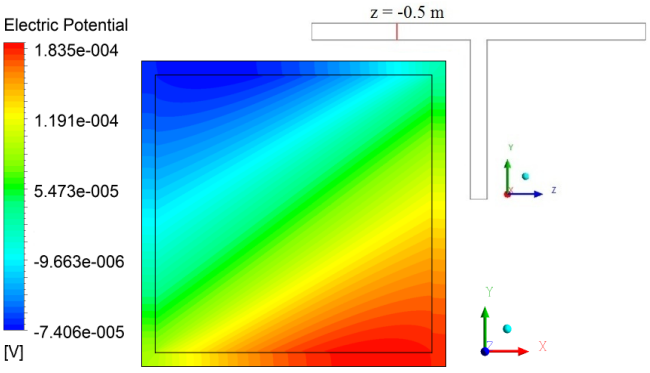

(b) Electric potential

Fig. 7 Current density and electric potential in the x-y plane at z = -0.5 m.

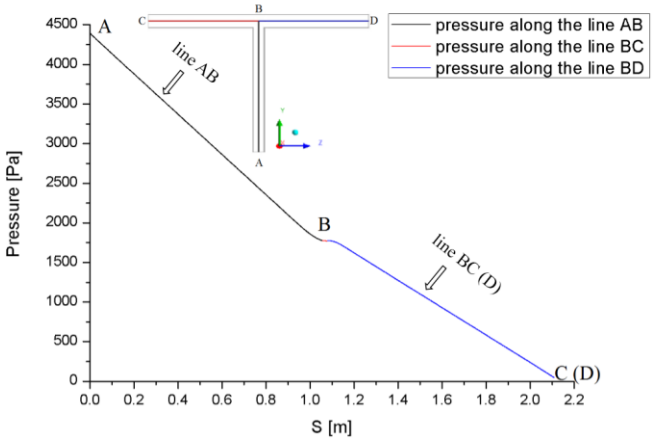

Fig. 8 Pressure distributions along the imaginary lines marked in the sub-figure. (Here, the two lines for pressure are coincident.)

decreases in the inflow and outflow channels. In the transition segment, the pressure change is smaller. More specifically, since higher average axial velocity of inflow channel yields higher current density leading to higher Lorentz force and pressure gradient, the pressure gradient of the inflow channel is the largest among that of the inflow and outflow channels.

IV. Conclusion

The current study investigates three-dimensional liquid metal (LM) magnetohydrodynamic (MHD) flows in a splitting duct under a uniform magnetic field with the use of CFX. The results of fully developed flows in the duct system, which consists of one inflow channel and two outflow channels are shown in the present study. Meanwhile, the

ISBN: 978-988-14048-9-3
ISSN: 2078-0958 (Print); ISSN: 2078-0966 (Online)

independency among the flow velocity, pressure gradient, current density and electric potential of the LM MHD duct flow is analyzed.

The simulation results show that the velocity jets are observed in the side layers, and the current flows diagonally due to the influence of the magnetic field, which forms an angle with the x-axis. In the inflow channel, higher pressure gradient is obtained due to higher average velocity distribution therein. In order to investigate the effects of different angle values of magnetic field with the x-axis on the flow distributions, the aim of the ongoing study is the comparison of the 3D LM MHD flow results with different angle values of magnetic field with the x-axis.

ACKNOWLEDGMENT

Yang Luo thanks Yiping Chen and Tiantian Li from CFD lab of Kyung Hee University, who support the author a lot in research field as well as normal life**.**

REFERENCES

[1] K. Messadek, M. Abdou, Experimental study of MHD flows in a prototypic inlet manifold section of the DCLL test blanket module, Magnetohydrodynamics 45 (2) (2009) 233-238.
[2] R. Stieglitz, L. Barleon, L. BüHler, S. Molokov, Magnetohydrodynamic flow through a right-angle bend in a strong magnetic field, Journal of Fluid Mechanics, 326 (1996) 91-123.
[3] I. R. Kirillov, C. B. Reed, L. N. Barleon and K. Miyazaki, Present understanding of MHD and heat transfer phenomena for liquid metal blankets, Fusion Engineering and Design, 27 (1995) 553-569.
[4] S. Cuevas, B. F. Picologlou, J. S. Walker and G. Talmage, Liquid-metal MHD flow in rectangular ducts with thin conducting or insulating walls: laminar and turbulent solutions, International Journal of Enginnering Science, 35 (5) (1997) 485-503.
[5] S. Aleksandrova and S. Molokov, The structure of parallel layers in steady two-dimensional magnetohydrodynamic flows in sudden duct expansions and contractions, Theoretical and Computational Fluid Dynamics, 26 (1-4) (2010) 29-35.
[6] P.G. Siddheshwar, U.S. Mahabaleswar, Effects of radiation and heat source on MHD flow of a viscoelastic liquid and heat transfer over a stretching sheet, International Journal of Non-Linear Mechanics, 40 (2005) 807-820.
[7] T. Zhou, Z. Yang, M. Ni, H. Chen, Code development and validation for analyzing liquid metal MHD flow in rectangular ducts, Fusion Engineering and design, 85 (2010) 1736-1741.
[8] I.D. Piazza, L. Buhler, Numerical simulation of Buoyant Magnetohydrodynamic flows using the CFX code, Forschungszentrum Karlsruhe Technik und Umwelt, Wissenschaftliche Berichte FZKA 6354, Forschungszentrum Karlsruhe, GmbH, 1999.
[9] J. Mao, H. Pan, Three-dimensional numerical simulation for magnetohydrodynamic flows in a staggered grid system, Fusion Engineering and Design, 2013 (88) 145-50.
[10] J. Reiman, L. Buhler, C. Mistrangelo, S. Molokov, Magneto-hydrodynamic issues of the HCLL blanket, Fusion Engineering and Design, 81 (2006) 625-629.
[11] M. Raw, Robustness of coupled algebraic multi-grid for the Navier–Stokes equations, AIAA Meeting Papers on Disc, A9618260, AIAA Paper 96-0297 (1996).
[12] W.Z. Shen, J.A. Michelsen, J.N. Sorensen, Improved Rhie-Chow interpolation for unsteady flow computations, AIAA Journal, 39 (12) (2001) 2406-2409.
[13] C.N. Kim, Magnetohydrodynamic flows entering the region of a flow channel insert in a duct, Fusion Engineering and Design, 89 (2014) 56-68.

ISBN: 978-988-14048-9-3
ISSN: 2078-0958 (Print); ISSN: 2078-0966 (Online)